

OPTIMAL POWER SYSTEMS FOR TACTICAL WHEELED VEHICLES

David Milner, Jarrett Goodell, Wilford Smith (SAIC, Inc.)

Mike Pozolo, Jason Ueda (U.S. Army RDECOM-TARDEC)

ABSTRACT

The next generation of tactical wheeled vehicles will require new and improved power system designs. As fuel prices continue to rise and as power draws become larger on tactical wheeled vehicles, the performance of the power system becomes more important. In this study, power system designs for Classes 3 through 8 wheeled vehicles are examined. Several power systems are chosen for analysis including series hybrid, parallel hybrid, CVT hybrid, and a traditional diesel engine power system. Power management algorithms are developed and implemented for each of the power systems. High fidelity models of these power systems are developed and integrated with vehicle models and power management algorithms in a front-end simulation tool built upon a standardized domain neutral, object-oriented, multi-domain modeling language that was established for component-oriented modeling of complex systems. With respect to mobility requirements, all power systems are chosen to either meet or exceed typical vehicle mobility requirements for existing Classes 3 through 8 vehicles. In order to determine optimal power systems for these tactical wheeled vehicles, trade studies are developed and performed. Variables used in the trade studies include the engine, transmission, battery, power management algorithm, and electric machines. Two main sets of trades are performed. The first is to determine an optimal set of power system components for each architecture (such as series, parallel, CVT, or traditional). The second set of trades is to determine which architecture is the best for each class of vehicle. For all trades, the output used to determine the optimal power system is fuel economy for the chosen duty cycle.

INTRODUCTION

The U.S. Army TACOM-TARDEC is investigating the means to improve the design of numerous Tactical Wheeled Vehicles (TWVs) with the use of new hybrid-electric power system architectures. For this purpose, an extensive set of models were created using modeling and simulation software to quantitatively compare and contrast the merits of various design upgrades for the vehicle's power systems. Specifically, a set of sixteen high-fidelity six-degree-of-freedom (6-DOF) vehicle models were developed representative of each class of vehicle investigated including classes 3, 6, 7, and 8 with each permutation of power system architecture including conventional diesel, series-hybrid, parallel-hybrid, and series-parallel combination with continuously variable transmission (CVT). The investigation involves determining the capacities required for each power train to enable each vehicle to meet its mobility performance requirements, followed by determining the relative improvements possible in mass/volume savings and fuel efficiency gains for each alternative design.

VEHICLE MODELS

Model Design Overview

Tactical wheeled vehicles for classes 3, 6, 7, and 8 were modeled as high-fidelity six-degree of freedom vehicle models with the modeling toolset. The vehicles model are comprised of fully integrated vehicle component systems including the vehicle chassis, independent pneumatic (compressible) wheels, suspension systems, complete power train, autonomous navigation controls, detailed terrain geometries and surfaces, and gravitational and air drag forces. Four power system models were modeled to represent each variation of power system design: conventional diesel, series-hybrid, parallel-hybrid, and series-hybrid combination with continuously variable transmission (CVT). The simulation of the models consists of calculations for lateral and longitudinal wheel slip, traction and normal terrain-wheel forces, suspension forces and deflections, power system loads, 6-DOF chassis motion, etc. The model accounts for all force and motion interactions between the wheels, suspension system, and the chassis. Figure 1 shows the top level of one vehicle model with representations for the complete vehicle structure, power systems, and path navigation control systems. The figure also shows a sample 3-D graphical rendering of one vehicle model for the FMTV 1083 A1 (Class 7) vehicle.

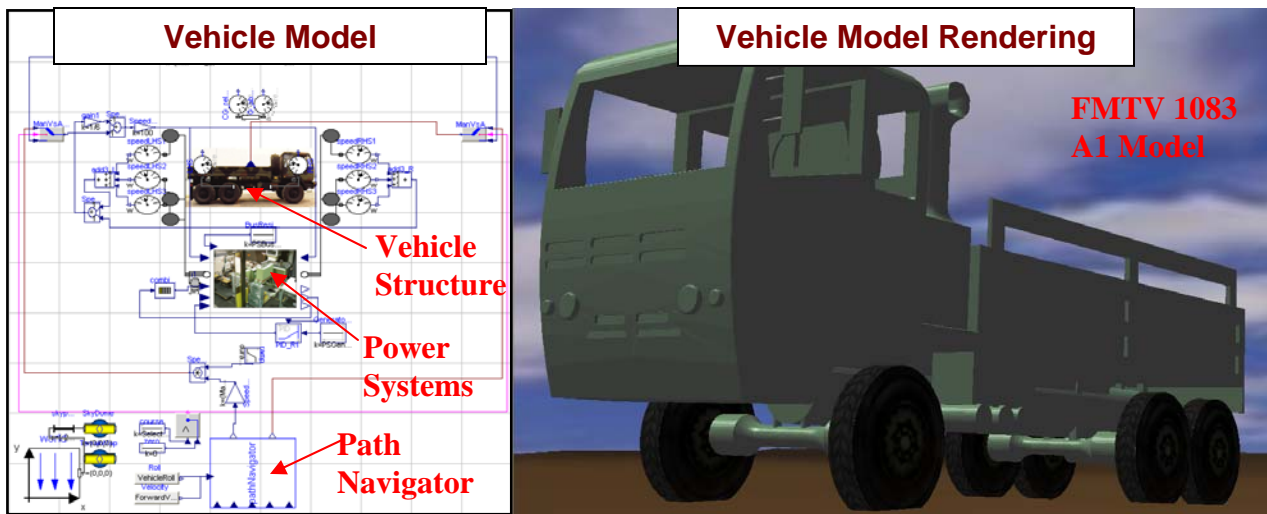


Figure 1: Top-Level View of Vehicle Model (left) and Graphical Rendering of Vehicle (right)

Vehicle Configuration

The vehicle structure model was constructed in four, six, and eight-wheeled configurations representative of the classes of tactical wheeled vehicles investigated. Each of these configurations was given specifications per actual tactical wheeled vehicles as representative setups with which to evaluate the performance of each power system studied. Figure 2 shows the three variations of vehicle structure models and the vehicles that were loaded into each of those models: the Class 3 HMMWV M1113 and Class 6 FMTV M1078 A1 in the 4-Wheeled Structure, the FMTV M1083 A1R in the 6-Wheeled structure, and the HEMMT M1120 A4 in the 8-Wheeled Structure.

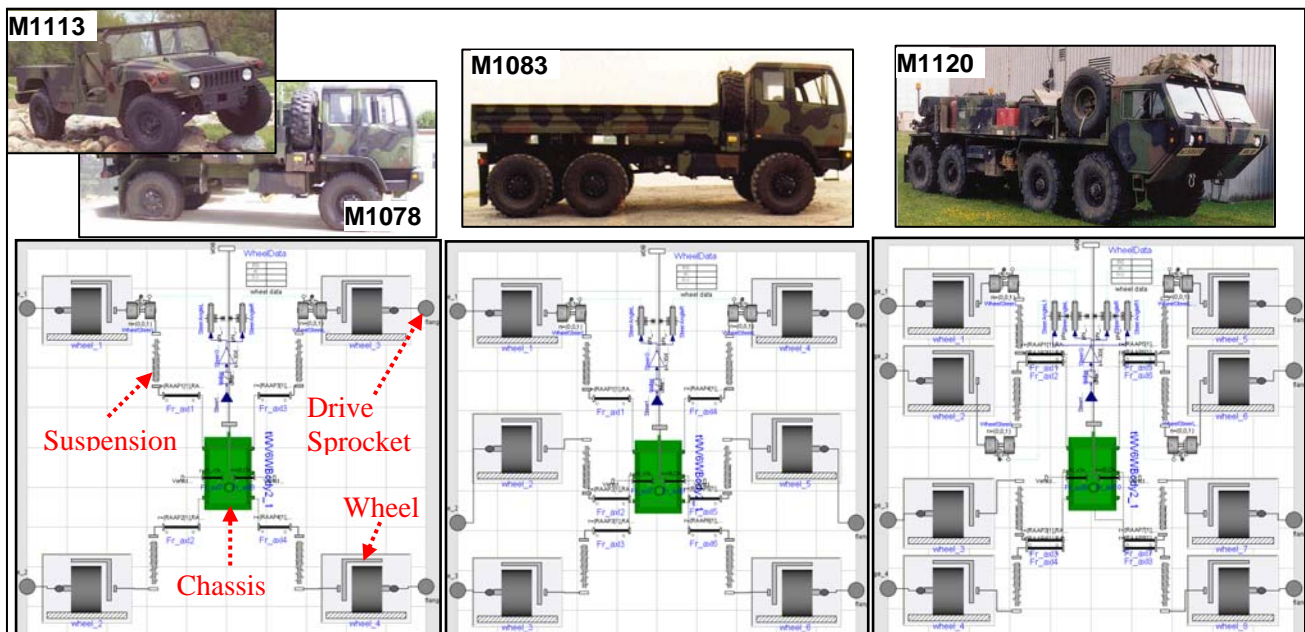


Figure 2: Vehicle Structure Models for 4-Wheeled Vehicle (left), 6-Wheeled Vehicle (middle), 8-Wheeled Vehicle (right)

Power System

The four power system architectures modeled included: conventional diesel, series-hybrid, parallel-hybrid, and series-parallel hybrid combination with continuously variable transmission (CVT); all of these are shown schematically in Figure 3. The conventional diesel power system has one primary source of power, a diesel engine, which is mechanically connected through a transmission to provide power to the vehicle's wheels; it is used throughout the army's current fleet of vehicles. The series hybrid power system includes two primary

sources of power, a diesel engine and a battery, which are electrically connected to motors that provide power to the vehicle's wheels. The series hybrid's engine can be relatively smaller and can be maintained at its point of optimal fuel efficiency, and its motor/generator system can store energy normally lost during braking to provide better fuel efficiency than that of the conventional diesel power system. The parallel hybrid power system also includes two primary sources of power, a diesel engine and a battery, but the engine is still mechanically connected through a transmission to provide power to the vehicle's wheels. The parallel hybrid's two power sources allows use of smaller and more fuel efficient engines, and its generator system stores energy normally lost during braking to provide better fuel efficiency than that of a conventional diesel power system. The series-parallel combination hybrid has the same two sources of power but with the engine mechanically connected through a planetary gear set and motor(s) to provide power to the wheels. The series-parallel can have a smaller engine than the conventional diesel and can be maintained close to its point of optimal fuel efficiency by control of its speed through direct commands to the relative speeds of the planetary gear set through control of the accompanying generator. Thus, all of the hybrid-electric power systems could provide improved mass and space savings relative to the conventional diesel by allowing use of smaller engines and other components, and could also provide improved fuel efficiencies for the vehicles.

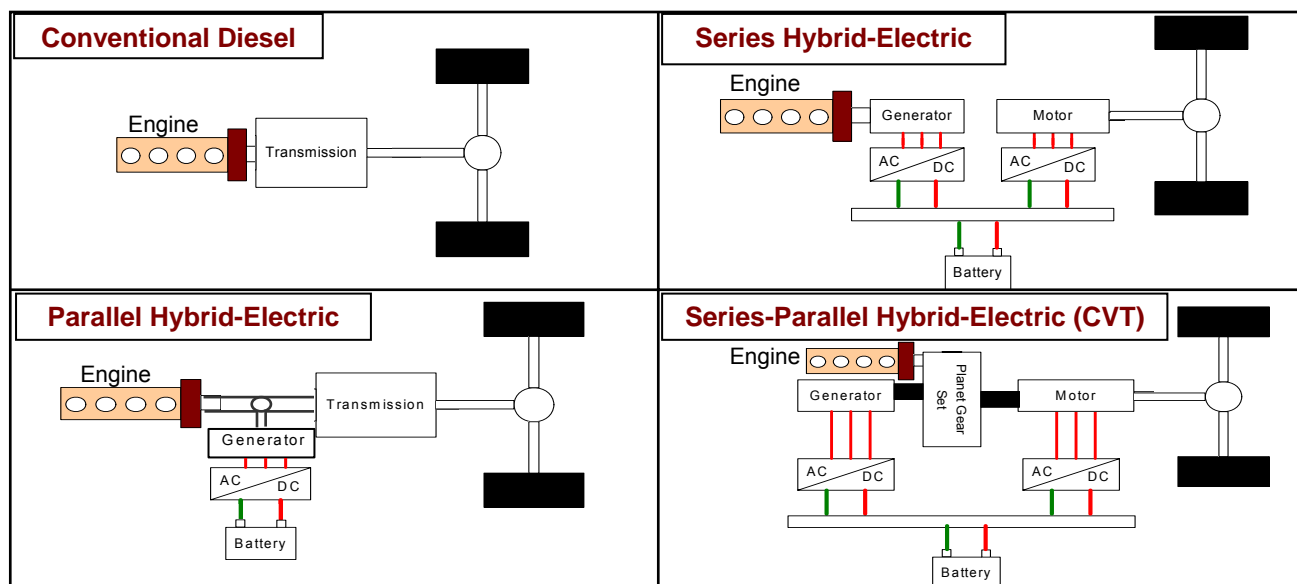


Figure 3: Power System Architectures

The power system models for these architectures were constructed with both the simulation software's electrical component library and custom code including batteries, engines, generators, motors, transmissions, and brakes. The models for the conventional diesel and series hybrid-electric power system are shown in Figure 4, while the models for the parallel and series-parallel hybrid-electric power systems are shown in Figure 5. The battery is designed as an equivalent circuit of a Lithium Ion battery, and includes state-of-charge (SOC) and temperature-dependence functions for its resistors, capacitors, and voltage source parameters. The engine is comprised of a torque-speed lookup table linked to an engine shaft and lookup table calculations for engine brake specific fuel consumption. The motors and generators calculate electromotive torques and apply them to rotational inertias that are linked to the final drives of each wheel. The transmission provides torque and speed scaling between drive train components. The brakes provide rotational friction for controlled braking when necessary. The power system is controlled directly from path navigation control outputs combined with algorithms for managing the engine speed and battery SOC in the appropriate hybrid-electric systems.

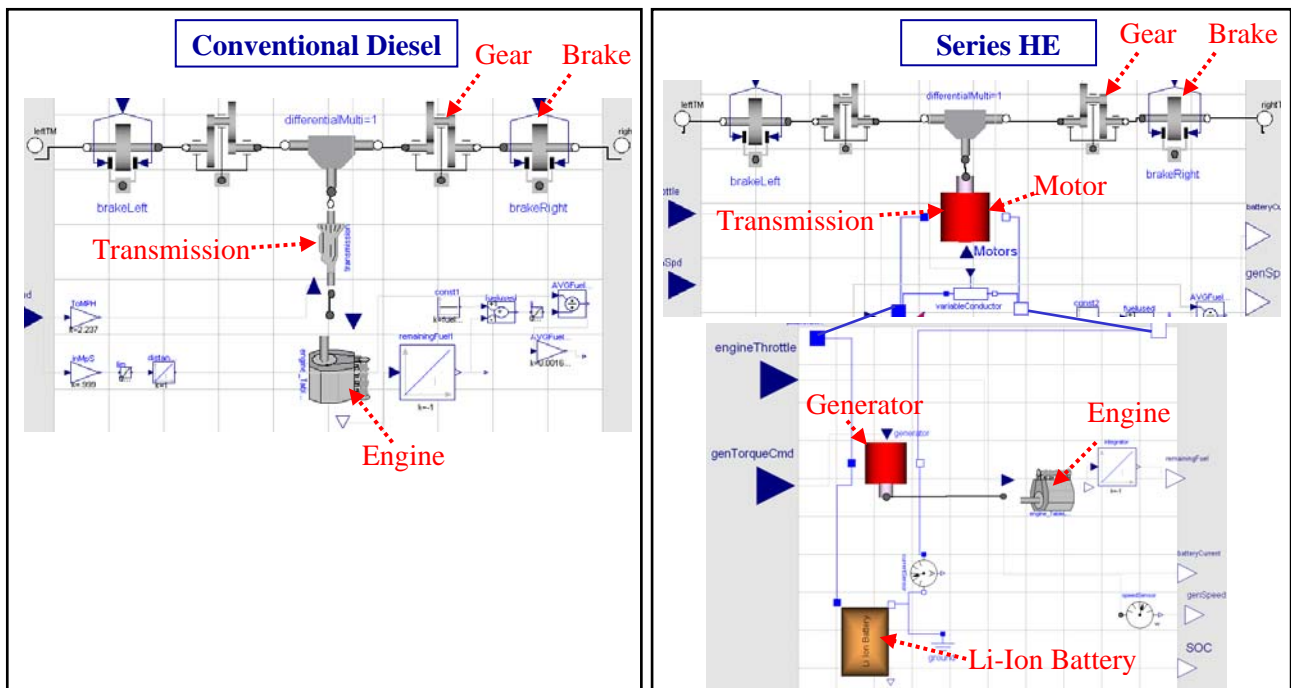


Figure 4: Power System Models of Conventional Diesel (left) and Series Hybrid-Electric (right)

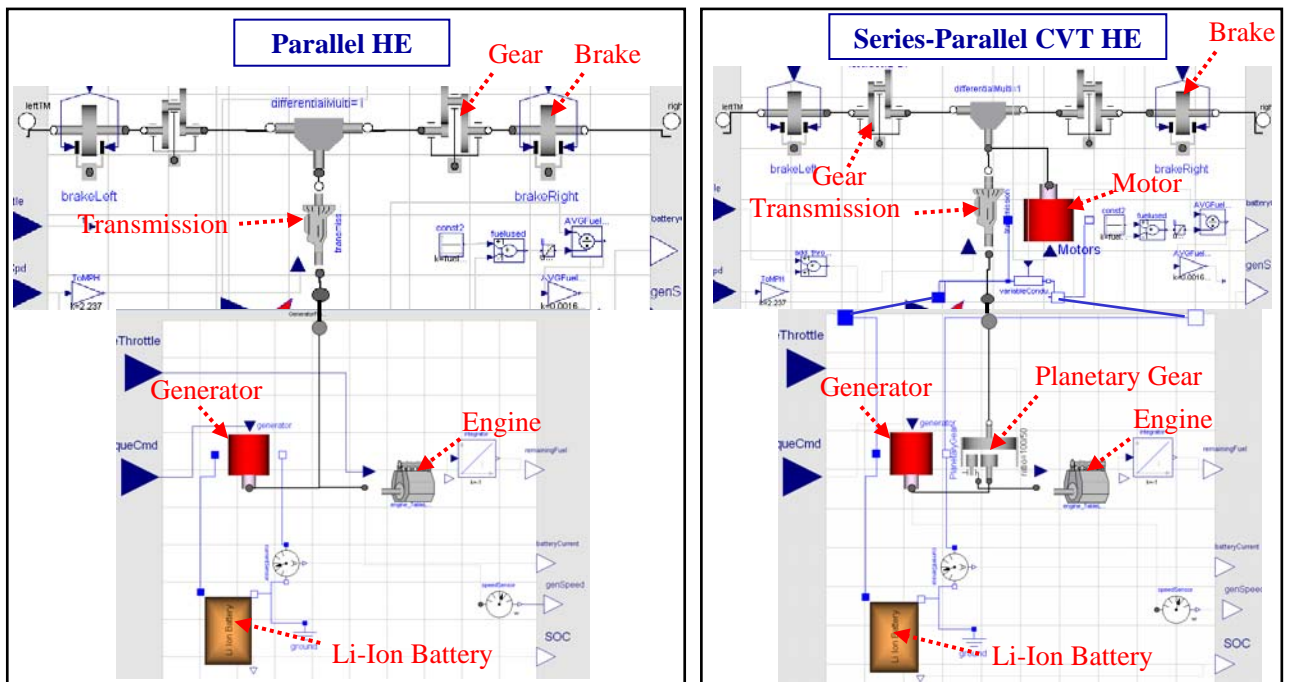


Figure 5: Power System Models of Parallel Hybrid-Electric (left) and Series-Parallel Hybrid-Electric with Continuously Variable Transmission (right)

Wheels

The wheels of the vehicle model were designed to encompass both on-road and off-road mobility calculations for the vehicle model using an empirical design. The wheel model was comprised of a compressible pneumatic tire mass with a primary rotational degree of freedom about its hub mass that was fixed to the hub end of the suspension. The power train provides torque directly to the wheel's rotating tire. The resultant forces acting upon the wheel model includes empirical formulations of both on-road (paved surfaces) and off-road (soft soil) terrain-wheel force calculations; the on-road forces were based upon the interpolated force-slip curves for normal tire loads, and the off-road forces were based upon off-road terrain-tire force calculations

presented in Wong¹⁵, with simplifications based upon equations from Shibly¹³. The model performs all transformation calculations included for all forces & coordinate frames of the wheel's connection points. The resultant forces are propagated through the suspension to the integrated vehicle model.

The forces acting upon the contact point for on-road conditions were calculated based upon both the deflection of the equivalent terrain-wheel contact point, the stiffness/damping characteristics of the tire surface, and empirically derived force-slip curves based on nominal (expected) loads for typical truck tires. The longitudinal and lateral terrain-wheel forces were calculated uniquely for each wheel by interpolating between two representative force-slip curves for these tires for the normal load on the wheel and the instantaneous *Slip* of the tire. These force-slip curves were defined in the model based upon a curve-fit for specific features of the curves including zero slip, slip of the maximum tire force, maximum longitudinal tire force, slip at sliding, and tire force at sliding as indicated in Figure 6. The *Slip* is the negative difference between the speed of the center of the wheel (V) and the speed of the wheel at the point of contact with the road all divided by the speed of the wheel, or wheel rotational speed multiplied by the wheel radius ($\omega \cdot R$).

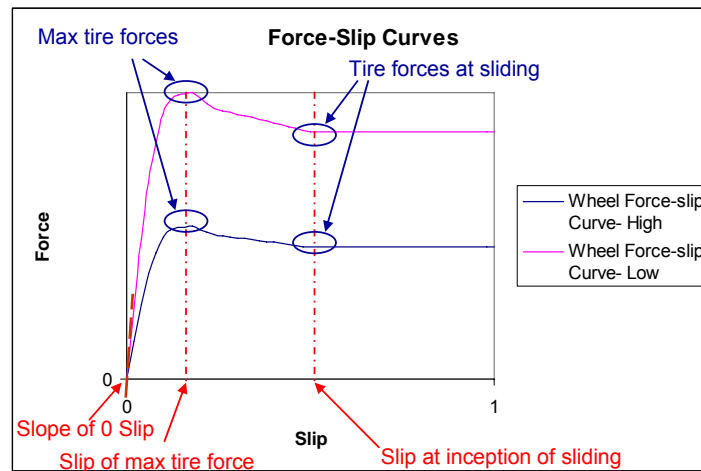


Figure 6: Force-Slip Curves Used for Calculating On-Road Tire Forces

The terrain-wheel forces for off-road vehicle traversal included resistive forces from soft-soil terrain-to-wheel interactions. These primary soft-soil resistive forces included longitudinal off-road forces F_{x-OR} , lateral off-road forces F_{y-OR} , and off-road torque M_{y-OR} all due to soil compression, shear, and bulldozing forces. The F_{x-OR} and M_{y-OR} off-road forces were calculated based upon the approximation of the pressure distribution acting upon the tire due to the sinkage z of the wheel into the ground. Shibly¹³ defined the normal pressure σ and shear force τ acting upon the tire with respect to the sinkage angle θ ; the sinkage angle is as a function of ground sinkage z that is determined in real time in the simulation depending on the normal load on the wheel and the characteristics of the off-road terrain as described in Wong¹⁵ for dry sand, sandy loam, clayey dirt, and snow. The assumption of a linear pressure distribution across the wheel-ground surface enabled the application of closed form solutions to be applied for the longitudinal force F_{x-OR} and lateral moment M_{y-OR} . All details for the terrain forces are provided in Milner¹².

Path Navigator

The automated path navigation system simulates driver inputs suitable for automated driving course negotiation. This is a waypoint-based navigation system that tracks the vehicle's position with respect to a predetermined course described by waypoints that define the desired trajectory for the vehicle to follow. The navigation system essentially tracks and actively minimizes the vehicle's body-fixed lateral and heading errors with respect to the desired path by providing either direct torque commands to the left and right side motors of the power system or steering angles to the wheels to successfully navigate a course. If the vehicle is skid-steered, the path navigator outputs torque commands to the left/right motors. Conversely, if the vehicle is Ackerman-steered, the path navigator supplies a steering angle to the front wheels. The model maintains smooth and stable steering inputs by using look-ahead functions to apply torque commands/steer angles to minimize heading error and lateral error as indicated in Figure 7. The model is currently loaded with five options of courses: Churchville B, Perryman A, Perryman 3, Perryman 1-Outer, a Combination Churchville/Perryman/Munson course, and a Flat plane course; the Churchville course is shown in Figure 7.

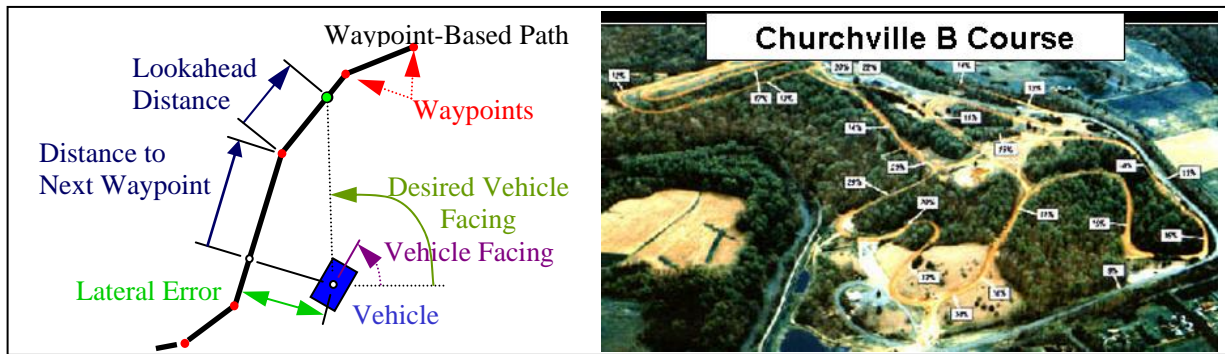


Figure 7: (a) a Discretized Waypoint-Based Path For the Desired Path (b) Churchville B Course

Model Visualization

Open source software was utilized to provide the graphical output for the simulation for the executable version of the model. For this purpose, the vehicle was visually rendered, converted to a mesh, and inserted in a graphics rendering tool. The tool shows the vehicle traversing the terrain based upon direct data inputs ported from the output of the executable simulation. The graphics script was setup with the rendered vehicle, and all three off-road terrains including the Churchville-B, Perryman, and Combination (Churchville/Perryman) courses.

Model Validation

The vehicle models were validated for their performance relative to experimental data. The FMTV 1083 A1 vehicle model was run on a flat, dry, hard road with a full-throttle straight-line acceleration from 0 to 50 mph and compared with data for the same vehicle conducting the same acceleration run. The test and simulation was run with extra weight added to the cargo bed of the truck to achieve a total test weight of 32,080 lbs. The FMTV 1083A1 used for testing was a conventionally powered diesel power train including a 330 hp diesel engine, an automatic transmission, and a final drive ratio of 7.8. There were no accessory loads applied to the modeled and experimental engines. Figure 8 shows the modeled and actual vehicle speeds aligned well.

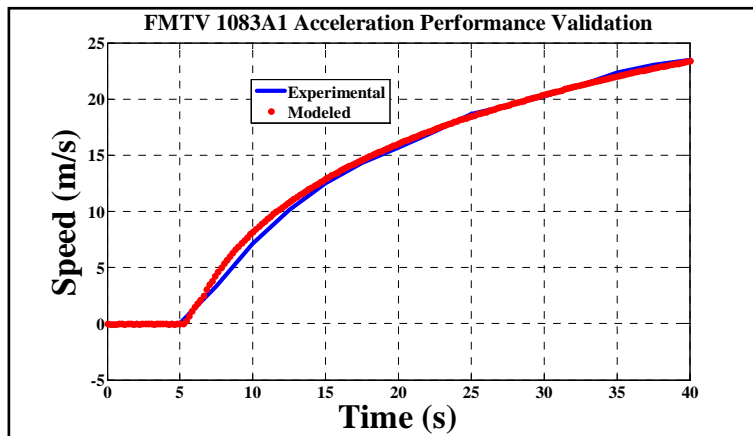


Figure 8: Conventional FMTV 1083A1 Validation

For a secondary measure of validation, the FMTV 1083 A1 vehicle model with the conventional power system was run on the Churchville-B off-road course. This course is a 3.7 mile closed loop, off-road course that contains grades up to 29% and has many turns; it is an accepted standard course for vehicle power train testing. The simulation used the clayey soil parameters per Wong¹⁵. The simulation results and experimental data were compared to verify the fuel consumption values for the course. At an average speed of 10 mph, the modeled vehicle achieved a fuel economy of 2.6 miles per gallon and the experimental vehicle achieved a fuel economy of 2.7 miles per gallon. This confirmed both the modeled and actual FMTV 1083 A1 vehicles required similar energy usage to traverse the Churchville terrain.

RESULTS

This validation check verified the modeled and actual FMTV 1083 A1 had similar acceleration performance and the model was therefore applicable as a baseline for comparison with the hybrid-electric vehicle models studied. Therefore, every model of the FMTV 1083 A1 vehicle including the conventional and all three hybrid-electric vehicles were run with similar loading characteristics and power system components that were sized to provide comparable performance. Figure 9 shows the performance of the conventional and all three hybrid-electric vehicles were comparable in straight-line full-throttle acceleration on road.

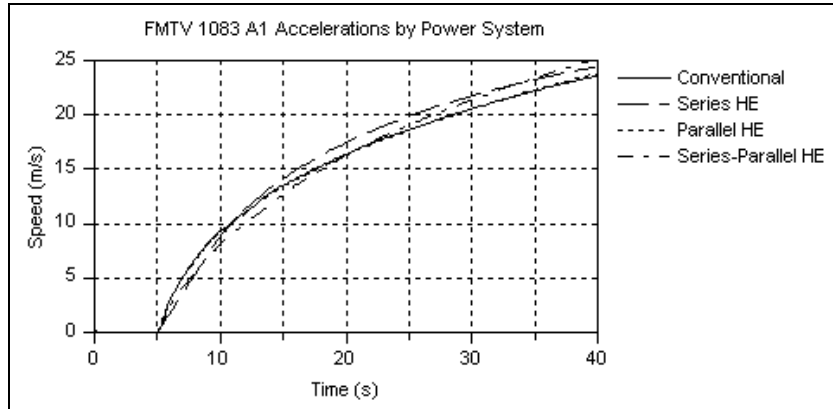


Figure 9: Conventional FMTV 1083A1 Validation

The FMTV 1083 A1 vehicle models with each power system was run on the Churchville B course at precisely 5.5 m/s to determine preliminary results of fuel economy with each type of power system architecture. The results shown in Figure 10 show the three hybrid-electric versions of the vehicle had improved fuel economy over the vehicle with the conventional power system. These adjusted values of fuel economy were determined by converting the battery's drop in state of charge from an initial level of 80% by an empirically determined ratio of 0.023 gallons/SOC% for the battery model used. The results are in Table 1.

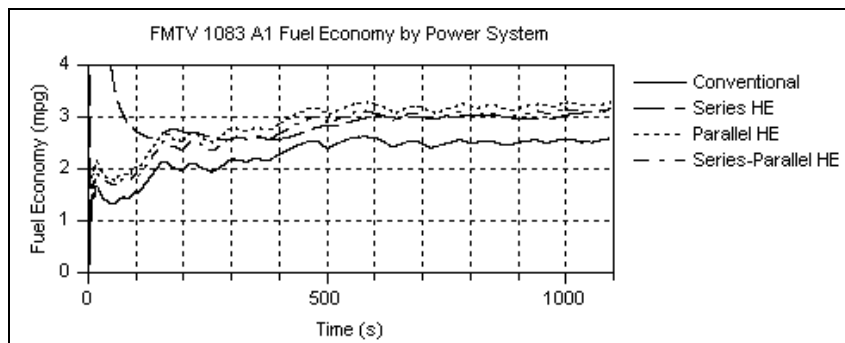


Figure 10: Fuel Economy Results for FMTV 1083 A1 on Churchville B by Power System

Table 1: Fuel Economy Results for FMTV 1083 A1 on Churchville B

Power System	Fuel Economy (mpg)	Battery End SOC (%)	Adjusted Fuel Economy (mpg)
Conventional Diesel	2.6	N/A	2.6
Series Hybrid	3.1	79.3	3.1
Parallel Hybrid	3.3	74.4	2.9
Series-Parallel Hybrid	3.2	81.0	3.3

CONCLUSIONS

Vehicle models were successfully developed for the conventional diesel and three hybrid-electric vehicles for four classes of tactical wheeled vehicles: Classes 3, 6, 7, and 8. The vehicle model for the conventional diesel FMTV 1083 A1 (Class 7) was validated to both on-road acceleration performance data and to fuel

consumption data for traversing the Churchville B course. The hybrid-electric versions of the FMTV 1083 A1 were configured to match the acceleration performance of the conventional diesel vehicle model. The preliminary results indicated the series and the parallel hybrid vehicles provided comparable performance and increased adjusted fuel economy results of 0.5 and 0.3 mpg respectively for traversing Churchville B compared with the conventional diesel power system. The Series-Parallel Hybrid power system provided an increased adjusted fuel economy result of 0.7 mpg for traversing Churchville B compared with the conventional diesel power system; this was the largest increase in fuel economy for these simulations. However, these results are only preliminary as more considerations will be made to these vehicle models. Further, the remaining three classes of vehicles still need to be evaluated. The results will be provided in a future report.

REFERENCES

- ¹Brudnak, M., Goodell, J., Compere, M., Simon, M., Smith, W., Wright, R., *Robust Control Techniques for State Tracking in the Presence of Variable Time Delays*, U.S. Army TARDEC, 2005
- ²Brudnak, M., Mohammad, S., Pozolo, M., Paul, V., Goodell, J., Compere, M., Smith, W., *Soldier/Hardware-in-the-loop Simulation-based Combat Vehicle Duty Cycle Measurement: Duty Cycle Experiment 2*, U.S. Army TARDEC, 2005
- ³Brudnak, M., Holtz, D., Meldrum, A., Mortsfield, T., Pozolo, Goodell, J., Shvartsman, A., Smith, W., *Virtual Combat Vehicle Experimentation for Duty Cycle Measurement*, U.S. Army TARDEC, 2007
- ⁴Compere, M., *Tracked Vehicle Mobility Modeling and Simulation*, September 2007
- ⁵Creedy, A.P., *Skid Steering of Wheeled and Tracked Vehicles-Analysis With Coulomb Friction Assumptions*, January 1985
- ⁶European Tyre School, *Testing and Evaluation of Tyre Like Component Part of Motor Vehicle* http://www.tut.fi/plastics/tyreschool/moduulit/moduuli_8/hypertext_1/index.html, 1999
- ⁷Frazer, William C., Griffin, Douglas R., *Final Report Broad Industry Announcement No. 15820 Platform Attribute Demonstration for the Future Combat System Performance Test Phase of the Hybrid Electric Drive for the Family of Medium Tactical Vehicles* US Army Aberdeen Test Center Aberdeen Proving Ground, MD February 2004.
- ⁸Lacomb, J., *Tire Model For Simulations of Vehicle Motion on High and Low Friction Road Surfaces*, Proceedings of the 2000 Winter Simulation Conference J.A. Joines, R.R. Barton, K Kang, and P.A. Fishwick, eds., p 1025-1034 Hanover, 2000
- ⁹Milner, D, Goodell J., Smith W., Tanner B.; *Work Directive AN Final Report - Advanced Vehicle Modeling and Simulation, Power and Energy Program Hardware In-The-Loop System Integration Laboratory*, U.S Army RDECOM TARDEC., April 30, 2008.
- ¹⁰Nunez, Patrick, Smith, Wilford, *Power and Energy Computational Models for the Design and Simulation of Hybrid-Electric Combat Vehicles*, U.S. Army TARDEC, 2008
- ¹¹Saarilahti, M., *Development of a Protocol for Ecoefficient Wood Harvesting on Sensitive Sites (Ecowood), Soil Interaction Model*, University of Helsinki, December 2002
- ¹²SAIC, *Power and Energy Word Directive 8 Final Report*. January 2006
- ¹³Shibly H., Iagnemma K., Dubowsky, S., *An Equivalent Soil Mechanics Formulation for Rigid Wheels in Deformable Terrain, With Application to Planetary Exploration Rovers*, Journal of Terramechanics 42 (2005) 1-13. Cambridge MA, July 2004
- ¹⁴Smith, Nicholas D., *Understanding Parameters Influencing Tire Modeling*, Colorado State University, 2003
- ¹⁵Wong, *Theory of Ground Vehicles*, 3rd ed., John Wiley & Sons, NY, 2001

CONTACT

David Milner, Research Engineer
Science Applications International Corporation
404-248-1543
milnerd@saic.com